Supra-resonant wingbeats in insects

Ethan S. Wold[1*], Rundong Yang[2], James Lynch[2],
Ellen Liu[3], Nick Gravish[2], Simon Sponberg[1,3]

[1] School of Biological Sciences and School of Physics[3]
Georgia Institute of Technology, Atlanta, GA, 30332 USA
[2]Mechanical and Aerospace Engineering,
University of California San Diego, San Diego, CA 92161, USA

[*] To whom correspondence should be addressed; E-mail: ewold3@gatech.edu.

Abstract

Powering small-scale flapping flight is challenging, yet insects sustain exceptionally fast wingbeats with ease. Since insects act as tiny biomechanical resonators, tuning their wingbeat frequency to the resonant frequency of their springy thorax and wings could make them more efficient fliers. But operating at resonance poses control problems and potentially constrains wingbeat frequencies within and across species. Resonance may be particularly limiting for the many orders of insects that power flight with specialized muscles that activate in response to mechanical stretch. Here, we test whether insects operate at their resonant frequency. First, we extensively characterize bumblebees and find that they surprisingly flap well above their resonant frequency via interactions between stretch-activation and mechanical resonance. Modeling and robophysical experiments then show that resonance is actually a lower bound for rapid wingbeats in most insects because muscles only pull, not push. Supra-resonance emerges as a general principle of high-frequency flight across five orders of insects from moths to flies.

Among the four evolutionary lineages of flying organisms, insects uniquely produce rapid, powerful wingbeats at the centimeter scale from the low whir of a giant silkmoth to the near-kHz hum of a biting midge (Fig. 1a) (*1, 2*). Wingbeat frequency is a critical determinant of aerodynamic power production (*3–6*), but is only weakly predicted by body size at the species level. For example, bumblebees flap at 180 Hz (*7*), but bee-mimicking hawkmoths, *Hemaris diffinis* (*8*), flap at 60 Hz despite being nearly the same size. Resonance is a popular explanation for this many-to-one mapping between body size and wingbeat frequency. Most insects fly by deforming an elastic exoskeleton with ultrafast flight muscles (*9–15*). Flapping at their resonant

frequency theoretically allows for the costs of rapid wing acceleration to be offset by elastic energy storage, but at the expense of frequency modulation capacity. While wing-clipping experiments (*3, 16*) and models (*9, 17*) point to insects being resonant, it is an unresolved question whether insects flap at resonance. Slow-flapping ($<$100 Hz), synchronous insects like moths may not be overly restricted by resonance because their wingbeats are paced by time-periodic neural signals, which can match or exceed the resonant frequency. However, resonance may be particularly constraining for fast-flapping (typically $>$100 Hz) asynchronous insects that generate self-excited wingbeats with specialized muscles that activate in response to mechanical stretch (*18–20*) (Fig. 1b). By combining new measurements of insect muscle and exoskeleton with models of 'spring-wing' dynamics, we investigate whether insects flap at resonance across taxa and flight mode, and if not, what timescales set their wingbeat frequencies.

Bumblebees flap above their resonance frequency

First, we focus our attention on the bumblebee, whose flight kinematics, morphology, and behavior have been characterized in detail. Using materials testing in the context of a 'spring-wing' model of an insect's elastic thorax, and the inertial and aerodynamic forces acting on the wing (*8, 10, 11, 20*), we demonstrate that asynchronous bumblebees flap above their resonant frequency (Fig. 1c-d). We estimated the resonance frequency of *Bombus impatiens*, by combining measurements of bulk thoracic stiffness with estimates of wing inertia and wing-hinge transmission ratio. The bumblebee's undamped resonant frequency (f_n) is a function of the measured thorax stiffness (k), the wing hinge transmission ratio (T , the ratio of angular wing displacement to muscle displacement with units $\mathrm{rad\ m^{-1}}$), and the inertia of the wings and added mass of air around the wing (I, see SI for extended description of all parameters),

$$f_n = \frac{1}{2\pi}\sqrt{\frac{k}{T^2 I}} \tag{1}$$

The elastic thorax and main flight power muscles (Fig. 1c) are in a parallel configuration that drive indirect actuation of the wing. We ignore series elasticity of the wing hinge, which is likely small and would widen but not alter the location of the undamped resonant frequency peak (*13*) (see Supplementary Discussion). We measured the isolated thorax stiffness of bumblebees using vibrational testing and found it to be 4.1 kN/m (see SI section 2.1) Setting all parameters from empirical measurements, we arrive at an undamped resonant frequency of $f_n = 94.9$ Hz, which is 44% lower than average wingbeat frequencies (180 Hz) (*7*) (Fig. 1d). Our measured thorax elasticity does not take into account active stiffness contributed by the flight muscles. Since the upstroke and downstroke muscles are antagonistic, when one contracts the other is stretched under near-tetanic activation. We estimate, conservatively, that active muscle stiffness is equal to the summed stiffness of both pairs of flight muscles, increasing the total thoracic stiffness to $6.4\ \mathrm{kN/m}$ and the resonant frequency to 102 Hz (*21*) when considering stiffness contributions from exoskeleton and active muscle. Propagating error in the three parameters k, T, and I, we find that supra-resonant bumblebee wingbeats are robust to reasonable measurement error in

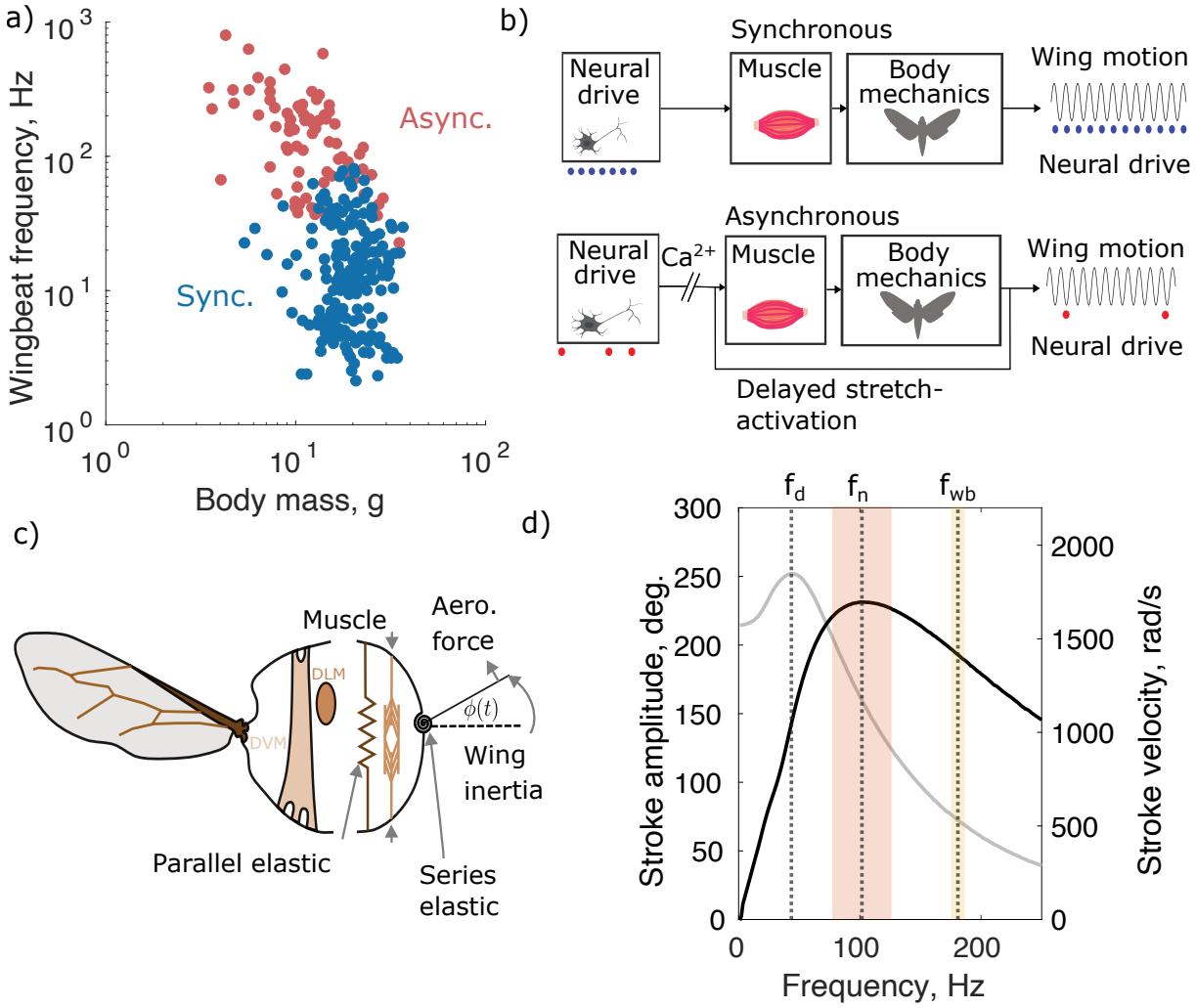

Figure 1: a). The division between synchronous and asynchronous insects helps explain the wide variation in insect wingbeat frequency. Data replotted from (*1*, *2*). b) Insects with synchronous muscle produce wingbeats at a frequency set by the neural drive to the flight muscles (blue dots). Insects with asynchronous muscle produce faster wingbeats that are decoupled in frequency from the underlying neural drive (red dots). c) Schematic of a bumblebee showing flight muscle anatomy on the left, and a biomechanical model on the right. d) Simulated displacement resonance curve (grey) and velocity resonance curve (black) of a bumblebee, assuming a sinusoidal forcing. Displacement resonant frequency (f_d) and velocity resonant frequency (f_n) are both below wingbeat frequency (f_{wb}). Orange and yellow bars show 95% confidence intervals of the mean for velocity resonance and wingbeat frequencies respectively.

thorax or wing properties, resulting in resonant frequencies ranging from 76 to 124 Hz (Fig. 1d).

We can also reverse the analysis to ask what thorax stiffness is necessary for wingbeats to be at the resonance frequency. This would require a stiffness of $21\ \mathrm{kN/m}$, which is beyond the largest stiffness that we measured and far exceeds any comparable stiffness measurements ($\approx$ 2 kN/m) (*15, 22*). Incorporating the effects of aerodynamic force production or internal thoracic damping into the resonance calculation can only further depress the estimated resonant frequency below wingbeat frequency (i.e. damped displacement resonance) (*8, 11*). More complex resonant models could create nonlinear resonance at higher harmonics, but we are interested here in the fundamental resonance from the exchange of inertial and elastic energy during the wingstroke. Thus, in the absence of evidence that substantial elasticity is missing from our measurements, we conclude that bumblebees are supra-resonant.

Stretch-activated dynamics of asynchronous muscle

The discrepancy between bumblebee resonant and wingbeat frequencies motivated us to consider how the physiological process of stretch-activation in muscle can enable supra-resonant flight in asynchronous insects. Asynchronous muscle generates active force in response to a rapid stretch. This mechanical stretch-activation was measured previously by stretch-hold experiments (*18–20, 23*) (Fig. 2a-b). The force response of isolated insect flight muscle to a step length change under tetanic activation has a shape that is composed of four phases (*24*) (Fig. 2c). The first two phases are fast, associated with the viscoelastic response of the muscle tissue. The slower third and fourth phases comprise the delayed stretch activation (dSA) force, which can be described with a single characteristic timescale, t_o (the time taken to achieve peak dSA force after the end of stretch (*20*)), and a constant, κ, the ratio of the rates of force decay (r_4) to force rise (r_3) (Fig. 2d). An analogous process, delayed shortening de-activation (dSD) occurs following rapid shortening (Fig. 2e, g) and is the inverse of dSA. We hypothesized that an asynchronous insect can flap above resonance if its t_o is sufficiently fast with respect to its natural period, the reciprocal of natural frequency ($T_n = f_n^{-1}$). In this case the resulting wingbeat frequency is set not just by the resonant mechanics, but by a combination of muscular (t_o) and mechanical (T_n) timescales.

To measure a bumblebee's dSA timescale under typical flight conditions, we had to conduct new stretch-hold experiments on isolated *B. impatiens* DLMs at the a realistic flight temperature of 40° C (*25, 26*) (Fig. 2a-e). While some measurements of bumblebee stretch-activation exist, we are the first to make them in intact whole muscle at a realistic body temperature. We measured the bumblebee stretch-activation timescale, t_o, to be 4.4 ± 1.0 ms, nearly the duration of an entire wingbeat, which did not change depending on muscle length at the onset of stretch (Fig. 2f-h). This value of t_o is somewhat faster than the only comparable characterizations in bumblebees at lower temperatures (≈ 5 ms) (*21, 27*), which may be because dSA rate kinetics are known to speed up with temperature (*23*). It is also substantially slower than the $\approx$ 2.5 ms necessary for dSA alone to drive 180 Hz wingbeats in response to stretch (the duration of

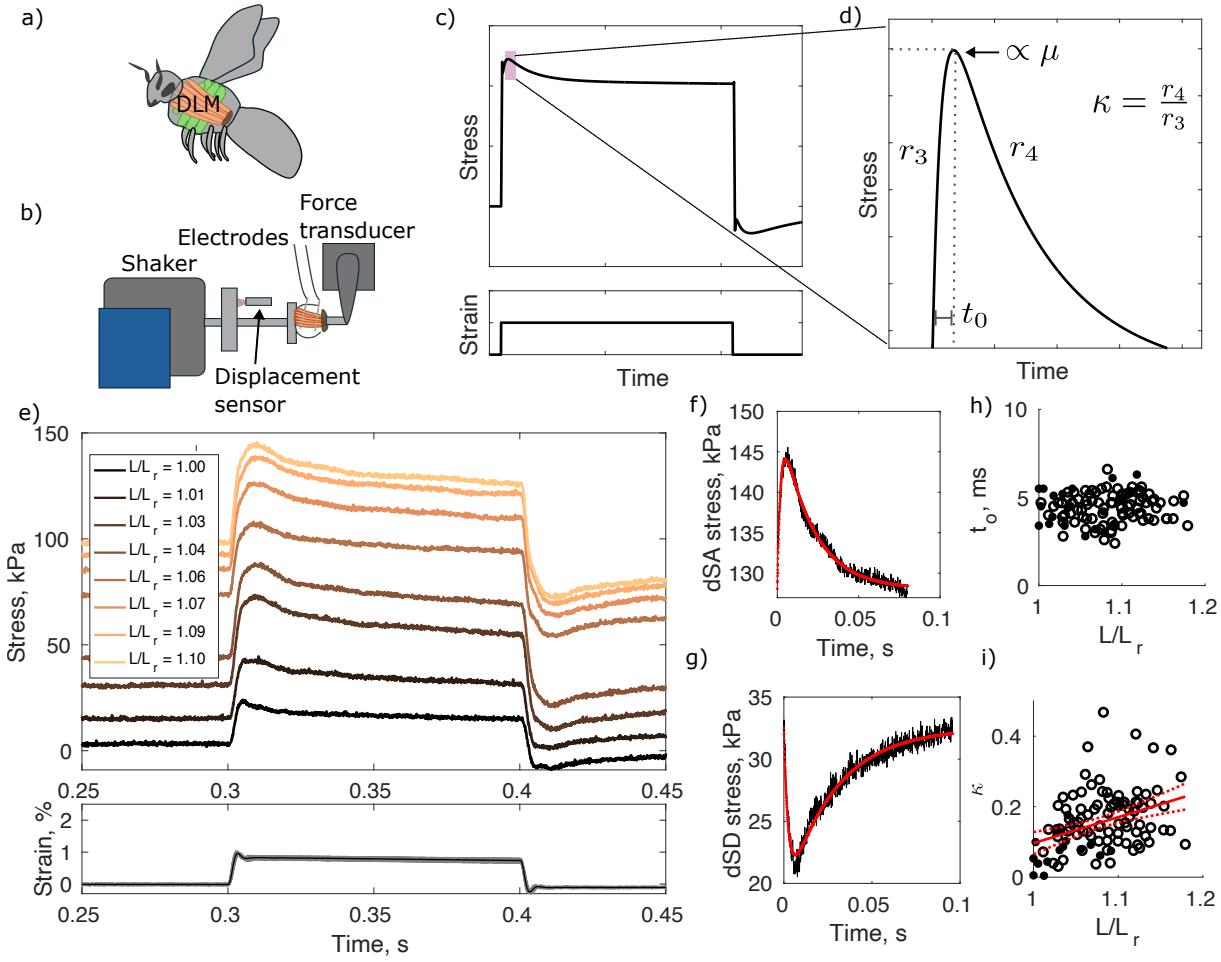

Figure 2: a). Location of the DLM (downstroke) muscles in a bumblebee. b). Schematic of muscle physiology apparatus used to apply step strains along the line-of-action of the DLM under tetanic stimulation. c). Zoomed out cartoon of a single stretch-hold-release-hold trial with purple bar blown up in panel d) Phases three and four of the dSA response, with corresponding rates of force rise (r_3) and force decay (r_4) notated. t_o is the time until peak dSA force is reached, and κ is the ratio of r_4 to r_3. μ is proportional to the height of the dSA response. e) dSA characterization experiments from a single individual. A 1% stretch was applied under tetanic stimulation at multiple starting lengths. f) dSA phases 3 and 4 from a single trial from a single individual. Red line denotes a double-exponential fit. g). dSD phases 3 and 4 from a single trial from a single individual. h) t_o computed across all individuals at all starting lengths (n=10 individuals). i) κ computed across all individuals at all starting lengths. Closed and open circles correspond to dSA and dSD measurements respectively. Red line shows a linear regression with 95% confidence intervals.

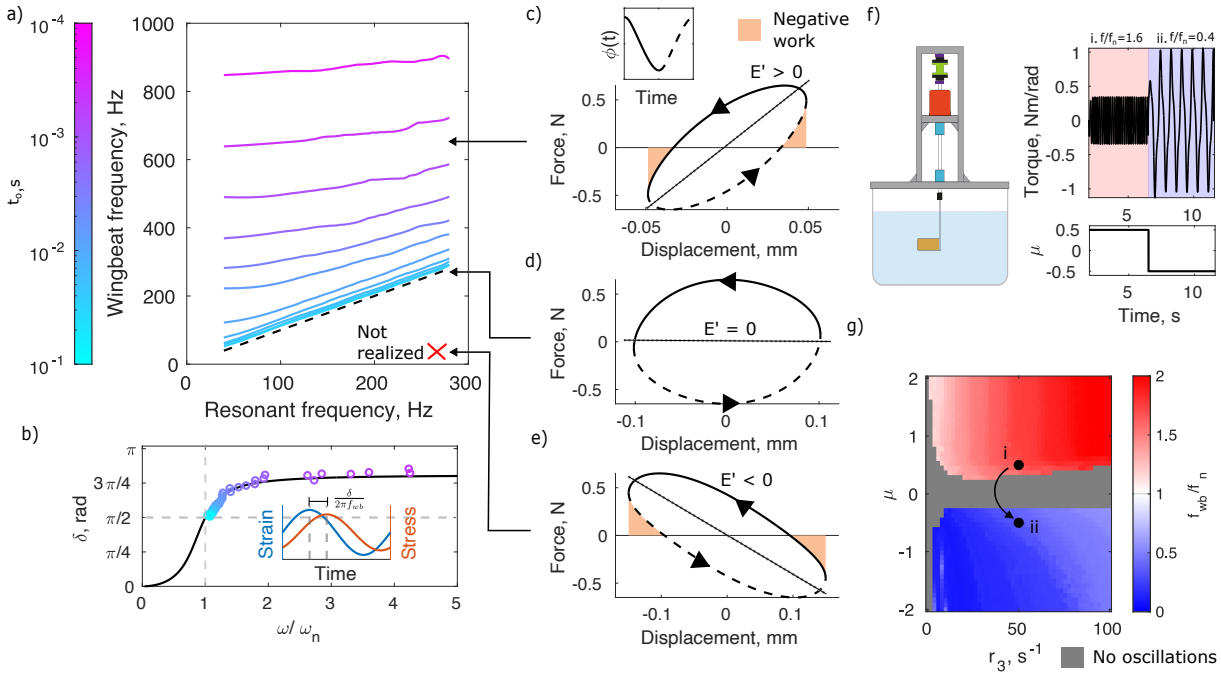

Figure 3: a). Parameter space of emergent wingbeats over a wide set of t_o and T_n that encompasses the physiological range for most insects. For any fixed value of t_o, there exists a linear relationship between resonant and emergent frequencies. At large t_o, this linear relationship collapses onto the equivalency line. As t_o decreases, wingbeat frequencies become supra-resonant, and increasingly independent of resonant frequency. Every point in simulation has been normalized such that steady-state peak-to-peak stroke amplitudes match bumblebee *in-vivo* conditions. b). Phase lag between stress and strain as a function of normalized frequency. Black line shows phase for a synchronous insect and colored dots show predictions from the asynchronous model for varying t_o, with the same color scale as in panel a). c-e). Work loop in force-displacement space for operation above (c), at (d), and below (e) resonance. Dotted lines correspond to upstroke and solid lines correspond to downstroke. At resonance, no negative work is required of the flight muscle. Above and below resonance, negative work is done in the second half and first half of each half-stroke, respectively. f). Robophysical experiment where the sign of the dSA force is changed from positive to negative, causing oscillations to transition from supra-resonant to sub-resonant. g). Space of asynchronous wingbeats in a robophysical flapper, demonstrating that transitions between sub- and supra-resonance occur only when the dSA force sign changes (i.e. across the $\mu = 0$ boundary). Parameter values corresponding to the transition in f). are shown by the arrow from i. to ii.

downstroke after being stretched during upstroke). The ratio of rates, κ, was weakly correlated with resting muscle length and on average equal to 0.17±0.03 (Fig. 2i). Thus, the muscular stretch response is faster than the timescale of mechanical resonance.

Asynchronous insects flap at or above resonance

To test our hypothesis that a sufficiently fast stretch-activation timescale (i.e. t_o) can enable supra-resonant wingbeats, we developed a biophysical model of asynchronous muscle-driven resonant flight. We drive a 'spring-wing' model of the insect's thorax and wings (*8, 10, 11*) with a simplified description of stretch-activated muscle, rooted in our stretch-hold experiments in bumblebees (*20, 30*). Thus, we capture the essential dynamics of both stretch-activation and resonant mechanics.

The model consists of two coupled, second-order differential equations. The oscillatory dynamics of the wingstroke angle, $\phi(t)$ are parameterized by k_l, T, I, and an aerodynamic damping coefficient Γ (Eq. 2). The stretch feedback-driven muscle forcing (Eq. 3) is parameterized by t_o and κ (see Supplementary Methods section 1.6.2). There is one free parameter, μ, which can be set by matching the amplitude of the output wingbeats to free-flight bumblebee wingstroke amplitude. μ represents the strength of the dSA forcing and makes the dSA force *in-vivo* proportional to the height of the two-phase response of the muscle to rapid stretch (Fig. 2c-d). Because the forcing is entirely state dependent and not prescribed exogenously (e.g. by the nervous system) the system oscillates at an emergent frequency (See Supplementary Results 2.2).

$$I\ddot{\phi} + \Gamma|\dot{\phi}|\dot{\phi} + \frac{k_l}{T^2}\phi = \frac{\mu}{T}f_{dSA} \tag{2}$$

$$\ddot{f}_{dSA} + \alpha_2(t_o,\kappa)\dot{f}_{dSA} + \alpha_3(t_o,\kappa)f_{dSA} = -\alpha_3(t_o,\kappa)\dot{\phi} \tag{3}$$

Simulating Eqs. 2-3 and evaluating the resulting $\phi(t)$ wing stroke trajectories over a wide range of muscular and mechanical timescales (t_o and T_n) reveal that resonance is a lower bound on emergent wingbeat frequency (Fig. 3a). There exists a large region of parameter space in which asynchronous insects can flap significantly above resonance. Consistent with observations from modifying the wing inertia of insects (*3, 16, 31*), the resonance frequency of the insect increases as the emergent flapping frequency goes up, regardless of t_o (Fig. 3a). However, this does not mean that the flapping frequency is at resonance. Fast stretch-activation, low t_o, results in supra-resonant wingbeats, while slower t_o result in wingbeat frequencies that collapse onto the wingbeat-resonant frequency equivalency line. Thus, stretch-activated resonant systems are not constrained to resonance, and can oscillate supra-resonantly with the right combination of t_o and T_n. Using our measured flight muscle stretch-activation timescale, we estimate a bumblebee wingbeat frequency which exceeds resonance by 33%, in agreement with our experimental characterization of supra-resonance using thorax materials testing.

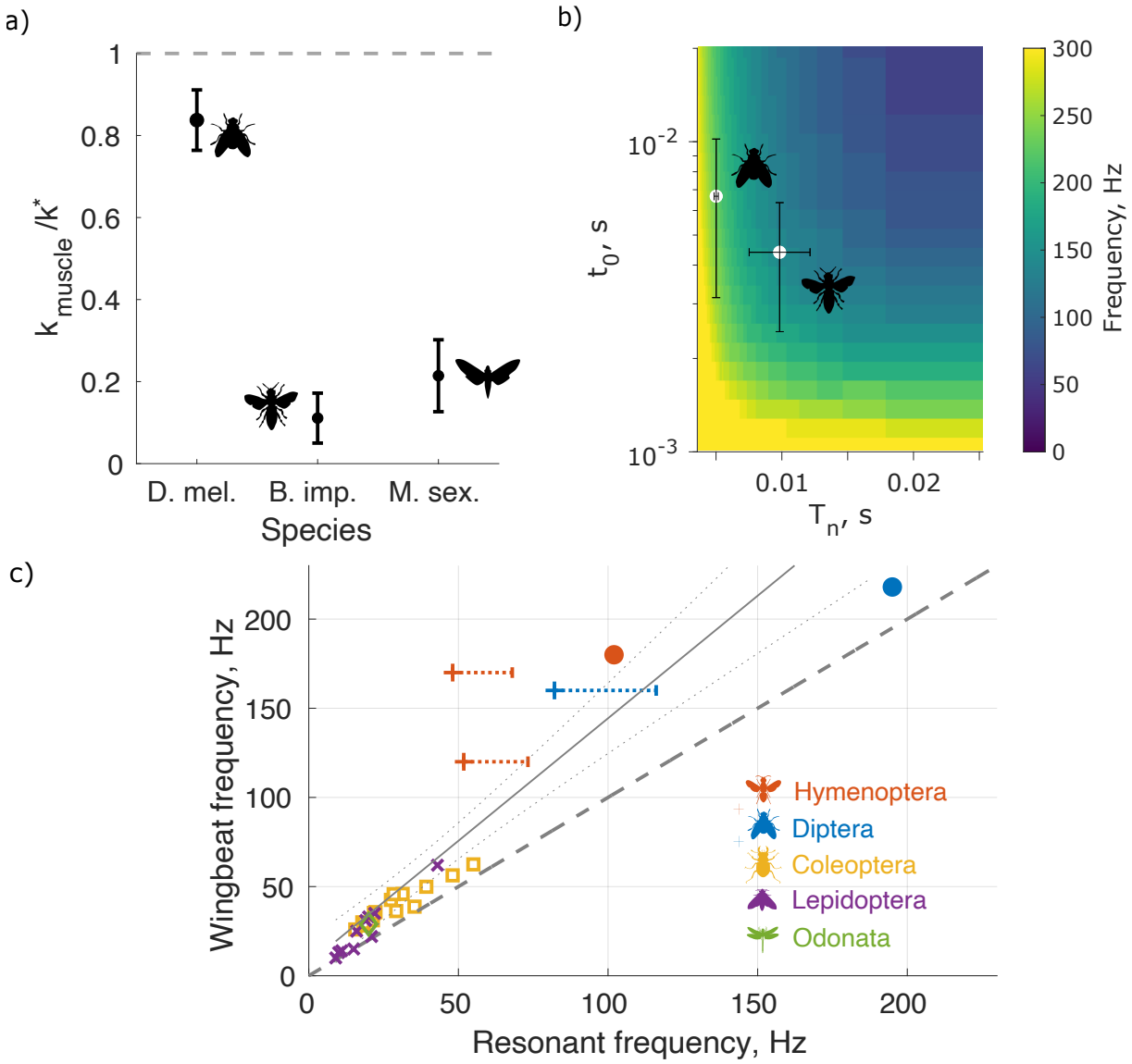

Figure 4: a). Fraction of perfectly resonant stiffness contributed by muscle alone for three insect species: fruitfly, bumblebee, and hawkmoth (*21, 28, 29*). b). Emergent asynchronous frequency space as a function of muscle time constant (t_o) and natural period (T_n). Both fruitfly and bumblebee achieve similar wingbeat frequencies with different combinations of t_o and T_n. c). Supra-resonant wingbeats across insects, compiling estimates from five insect orders. Markers - "$\times$" (*8*), "+" (*22*), square (*18*), and diamond (*17*) - represent data from different studies. Dots show data from the current study. Dotted line shows equivalence of wingbeat and resonant frequencies. Orange bars show resonant frequency ranges assuming exoskeleton stiffness underestimates total thorax stiffness (exoskeleton + muscle) by up to a factor of two. Solid grey line shows a linear regression through all points, with dotted grey 95% CI.

Muscle's asymmetry enforces supra-resonance

Why are asynchronous flappers apparently only able to flap at or above resonance? This constraint emerges from muscle producing a positive force in response to stretch (i.e. always 'pulling' and never 'pushing'), such that increases in muscle stress will always lag positive muscle strain (muscle extension) (Fig. 3b, inset). This phase lag is proportional to the stretch-activation timescale (t_o), but can never be below a quarter cycle ($\pi/2$ radians) because increasing t_o results in a frequency that asymptotes to resonance. As t_o increases, δ approaches $\pi/2$; as t_o decreases, δ approaches a maximum. Thus, stretch-activated wingbeats can never be sub-resonant, which would require $\delta < \pi/2$ (Fig. 3b, colored points). This contrasts with a synchronous insect that has neurally activated muscle, which can theoretically achieve $0 < \delta < \pi$ by modulating the timing of neural signals to the flight muscles (Fig. 3b, black line). This would be equivalent to activating the muscle such that it produces significant force in the half cycle prior to lengthening (*32–36*).

The necessity of asynchronous insects to be supra-resonant can be visualized in the workloop representation of muscle function, which visualizes muscle work output as the area enclosed in active force vs. displacement space (*37–40*). In this space, the effective storage modulus, E', of the workloop represents the elastic component of the total muscle force necessary to supply all energy requirements for flight (see Supplementary Results 2.3). $E' = 0$ represents perfect exchange between wing kinetic energy and thoracic elastic energy (i.e. $f_{wb} = f_n$) (Fig. 3d). $E' \neq 0$ represents non-resonant conditions where the thorax is either too stiff or not stiff enough with respect to the wingbeat frequency (Fig. 3c,e). The hysteresis of the loop is proportional to the phase lag δ between force and displacement. The resulting area within the loop is the effective loss modulus, E'', representing the mechancial energy generated by the muscle.

At steady-state, the muscle forcing $f_{dSA}(t)$ will always follow a counter-clockwise ellipse (negative loss modulus or positive net work) with a nonnegative storage modulus. This enforces a phase lag, δ, of $\pi/2 < \delta < \pi$ in stress with respect to strain. If the insect is supra-resonant, its muscle will produce negative work, dissipating energy, during the second half of each halfstroke while the wing is decelerating (Fig. 3c, shaded area). Muscle assisting in the slowing of the wing on each half cycle is only possible in a supra-resonant system, since the thoracic spring will not be stiff enough to absorb all of the wing's kinetic energy before it reaches its extremal positions. At resonance, the storage modulus of the muscle is identically zero and no negative work is required at any point in the wingbeat (Fig. 3d). Below resonance, an overly stiff thoracic spring would cause rapid wing acceleration that is counteracted by muscle dissipating energy in the acceleration phase of each half-stroke (Fig. 3e, shaded area). Thus, a sub-resonant asynchronous insect would have to generate negative work directly following stretch, which is incompatible with the polarity of muscular dSA force response. Muscles only pull, they do not push.

Supra- and sub-resonance realized through a robophysical model

While the physiological limitations of biological muscle limit oscillations to at or above resonance, engineered actuators are not necessarily limited to this regime. In contrast, they can push and pull. Following from the sub-resonant work loop (Fig. 3e), we predict that an engineered system with muscle dSA-like actuators that pushed instead of pulled should be able to realize sub-resonant asynchronous wingbeats. We demonstrate asynchronous sub-resonant oscillations in a dynamically scaled robophysical flapping wing by controlling a brushless DC motor with a velocity feedback-driven forcing analogous to dSA (Eqs. 2-3) (*30*). This system is also unable to oscillate below its resonant frequency, when controlled with a muscle-like dSA forcing (Fig. 3f, i.). However, by changing the sign of the dSA force such that a negative (i.e. pushing) force follows stretch, stable sub-resonant oscillations emerge that are bounded above by the resonance frequency (Fig. 3f, ii.). By systematically changing μ in the model that controls our roboflapper motor, we see the boundary of switching between supra- and sub-resonant behavior is at $\mu = 0$, where the sign of the dSA force flips (Fig. 3g). Thus, we demonstrate that the physiology and arrangement of antagonistic stretch-activated muscles in asynchronous insect thoraces constrain them to supra-resonant wingbeats.

Sub-resonance is realizable in some biological muscle-driven systems as well. For instance, unlike asynchronous insects, synchronous insects can, in theory, be sub-resonant. They could neurally activate their muscles at timings that would enable negative work production in the first part of each half-stroke. Practically, this would require the downstroke muscle (or a combination of muscles) to produce significant force during the beginning of upstroke, and vice versa. This would require either multiple downstroke or upstroke muscles or a large degree of coactivation which would likely reduce the production of useful work from the muscles. While we do not see such activation patterns in insects, they are common in terrestrial locomotion especially where multiple muscles operate in synergy at a joint or in a limb (*33–36, 41*). Indeed, some terrestrial animals like kangaroos are sub-resonant (*42*), but do not have to contend with the asynchronous muscle dynamics present in bumblebees or our robophysical flapper.

Supra- and sub-resonant systems also exhibit a key difference in how they modulate power output outside of the steady state. In a supra-resonant system, acceleration is muscle-driven and spring-assisted, with negative muscle work (dissipation) coinciding with the deceleration phase of the wingstroke (Fig. 3c). The muscle assists the spring. This enables supra-resonant systems to inject additional accelerative power via transient increases in agonist muscle force. However, in sub-resonant systems, acceleration is driven by the spring and braked by the agonist muscle (Fig. 3e). Positive power production is limited by the spring's capacity to return elastic energy and additional agonist muscle force would only decelerate the wing faster. Thus, an important benefit of supra-resonance for asynchronous insects may be to maintain the capacity to transiently boost wing acceleration via positive muscle power production in the first part of each half-stroke (Fig. 3c).

Two timescales pace asynchronous wingbeats

Having validated our model in bumblebees, we used recent characterizations of *Drosophila melanogaster* muscle stiffness and flight mechanics to show that this widely-studied fruitfly is also supra-resonant, although to a lesser degree than *B. impatiens*. *D. melanogaster* has more than three orders of magnitude less mass than a bumblebee, but paradoxically has a wingbeat frequency of around 200 Hz, which is very close to that of *B. impatiens* (*43*). Measurements of fruitfly delayed stretch activation timescale, t_0, range from 5-8 ms which is slower than our measured t_o for bumblebees (Fig. 2h) (*44*). We hypothesize that fruitflies have evolved a similar wingbeat frequency to bees despite being much smaller in part by having relatively slow stretch-activation in comparison to their natural period. Indeed, fruitfly wing inertia is roughly four orders of magnitude smaller than that of a bumblebee, which in isolation would suggest a resonant frequency far greater than ≈ 100 Hz we measured in bees.

To test this hypothesis, we first need an estimate of the bulk stiffness of the fruitfly thorax. While exoskeletal stiffness values for fruitflies have not been measured, functional stiffness in the fly thorax is thought to be dominated by active muscular elasticity, rather than parallel thoracic stiffness. This is due to fruitflies' combination of small wing inertia compared to bees, and asynchronous muscle which has much higher resting stiffness than synchronous muscle (*19, 21, 28, 45*). We quantify whether existing estimates of muscle elasticity alone are sufficient to estimate resonance frequency, by deriving a new metric describing the contribution of muscular elasticity to bulk thorax stiffness: the ratio of the active muscle stiffness k_{muscle} to the stiffness that would be required to drive perfectly resonant wingbeats, $k^* = (2\pi f_{wb})^2 T^2 I$ (Fig. 4a). This expression depends on nonlinear interactions between morphological (wing inertia, I), kinematic (wingbeat frequency, f_{wb}), and biomechanical (transmission ratio, T) parameters. It is not a simple function of body size. Bumblebees and moth thoraces are dominated by exoskeletal stiffness, which is in excess of muscular stiffness by at least three-fold yet their free flight frequencies are still above their undamped resonance. In contrast, *Drosophila* muscle does supply nearly all the elasticity needed to drive wingbeats close to resonance (Fig. 4a).

Armed with a stiffness estimate for *Drosophila* we can then apply the same approach we took with bumblebees to test if they operate at their resonant frequency. When we estimate *Drosophila* resonant and wingbeat frequencies using Eqs. 1-3, we find a predicted emergent wingbeat frequency (221 Hz) that is supra-resonant at 18% in excess of resonance (187 Hz) (Fig. 4b). Supra-resonance arises from a combination of a much larger transmission ratio (ratio of wingbeat angle change to muscle displacement) by virtue of small body size as well as slower stretch-activation (longer t_o). These frequencies are within the range of measured free-flight wingbeat frequencies. While series-elastic effects in moths and bees are not large enough to significantly impact our results (see Supplementary Discussion), high series-elastic compliance in *Drosophila*-scale flies may widen their resonance curves to the point where they can still achieve near-maximal resonant energy return while being supra-resonant (*13*). Thus, our modeling demonstrates how dSA causes a single frequency that exceeds f_n to emerge from a band of potentially equally efficient frequencies in insects with significant series compliance.

We find that bees and flies realize similar asynchronous wingbeat frequencies through different combinations of t_o and T_n while remaining slightly (flies) to significantly (bees) supra-resonant (Fig. 4b).

Supra-resonance as a general principle of insect flight

Our experimental and theoretical characterizations of resonance in bees and flies point to supra-resonance as a general principle of insect flight, but how broadly does it apply? Collating our results with the only other comparable characterizations of resonance (*17, 18, 22*), we show that supra-resonance applies to asynchronous bees, flies, and beetles, and synchronous moths. Even the dragonfly, a synchronous insect with a direct flight muscle architecture appears to operate above its resonance peak. This suggests that supra-resonance is not limited to insects with indirect flight muscles so long as there is some degree of elasticity in the muscles or wing hinge (*17*). Thus, our results demonstrate a general pattern of supra-resonant wingbeats in insects, with all insects included flapping at or above their resonant frequency. Insects generally fall on a line with slope > 1 (slope$= 1.32$, $p < 0.001$, $r^2 = 0.77$) but an intercept statistically indistinguishable from 0. Thus across taxa, insects maintain a roughly constant ratio of wingbeat to resonant frequency, with slower-flapping insects flapping extremely close to, but not below, resonance.

Interestingly, *Drosophila* lies closer to resonance than predicted by a line of best fit through all other species (slope$= 1.84$, $p < 0.001$, $r^2 = 0.80$), suggestive that higher frequency insects may not continue to experience a divergence between resonant and wingbeat frequencies. This makes sense in the context of its larger t_o compared to that of a bumblebee (*44*), despite being orders of magnitude less massive. In addition, smaller insects achieve roughly the same amplitude wingbeats with much smaller muscle displacements, resulting in a sharply increasing transmission ratio (driving a decrease in T_n) with size. Adaptations in wing hinge musculature and gearing (*2, 46*) may tune the transmission ratio and enable modulation of wingstroke parameters without changing wingbeat frequency. Thus, a combination of effects on t_o and T_n likely pushes millimeter-scale fliers closer to resonance than bees, making way for extreme kinematic and morphological adaptation to facilitate maneuverability (*47*).

Our results demonstrate that the physiology of asynchronous muscle activation under cyclic strain constrains many insects to operation at or above resonance, suggestive of a widespread advantage to supra-resonant flight. The apparent ubiquity of supra-resonant flight also demonstrates that resonance tuning is not necessary for insect flight systems. While smaller insects generally beat their wings faster and have higher resonant frequencies, competing biomechanical and physiological pressures from muscle, wing, and exoskeleton make perfectly resonant wingbeats a precarious target for selection. The capacity for supra-resonance widens the phenotypic space for successful flight, opening up the possibility of evolutionary tuning of insect resonant properties for control, efficiency, or speed (*8, 12, 48, 49*).

Operation above resonance may enable increased frequency-modulation capacity in asynchronous insects via modulation of resonant properties, such as during different buzzing modes in bees, or during sensory feedback driven maneuvers in flies (*31, 50*). For example, decreas-

ing the transmission ratio by keeping the wings retracted (such as during bumblebee defense buzzing) would drastically decrease the resonant period, and could easily result in a doubling of wingbeat frequency without any modification of muscle properties (Fig. 4b) (*51*). Such a mode of frequency modulation would not be possible if bumblebees had much faster muscle stretch activation kinetics (t_o), because the low-t_o region of the parameter space has a flat relationship between emergent and natural frequency (Fig. 3a, 4b). Similar modulation capacity in synchronous insects is possible by transient neurogenic frequency changes during perturbation recovery (*8, 12, 48*).

Temperature-dependent modulation of wingbeat frequency via changing stretch-activation time constants may be important in thermogenesis buzzing, or for insects that fly in cold conditions such as alpine honeybees (*52*). One unique challenge faced by insects at the size of a fruitfly and smaller is that they cannot maintain flight muscle temperatures significantly above ambient temperature. This temperature constraint may cause faster-flapping insects to have a slower t_o since stretch-activation timescales are known to be highly temperature-sensitive (*23, 53*). Modulation of wingbeat frequency by calcium-dependent potentiation of asynchronous muscle force may also be more effective above resonance (*54*). In general, our results suggest that the timescale of asynchronous muscle's stretch activated dynamics (t_o) and the timescale of the mechanics of resonant spring-wing thorax (T_n) are independent axes by which the emergent wingbeat frequency can change over long timescales by selection, or short timescales by phenotypic plasticity (Fig. 4b).

Asynchronous flight was a key evolutionary innovation that opened the possibility for superfast wingbeat frequencies, enabling insects to miniaturize and diversify. Contrary to the longstanding hypothesis of resonance tuning, our materials testing, muscle physiology, dynamical and robophysical modeling demonstrate that many asynchronous insects flap significantly above their resonant frequency. We highlight a mechanism for asynchronous supra-resonance: a tug-of-war between intrinsic physiological timescale of asynchronous muscle and the resonant mechanics of the thorax and wings. Supra-resonance also generalizes to multiple synchronous orders, despite their wingbeat frequency being determined neurally. Thus, supra-resonance is an underappreciated and widespread property of insect flight, that underscores the importance of balancing efficiency and agility across Earth's smallest aerial locomotors.

References

1. Dudley R. 2002 *The biomechanics of insect flight: form, function, evolution*. Princeton University Press.

2. Deora T, Gundiah N, Sane SP. 2017 Mechanics of the thorax in flies. *Journal of Experimental Biology* **220**, 1382–1395.

3. Greenewalt CH. 1960 The Wings of Insects and Birds as Mechanical Oscillators. *Proceedings of the American Philosophical Society* **104**, 605–611.

4. Dickinson MH, Lehmann FO, Chan WP. 1998 The control of mechanical power in insect flight. *American Zoologist* **38**, 718–728.

5. Aiello BR, Tan M, Bin Sikandar U, Alvey AJ, Bhinderwala B, Kimball KC, Barber JR, Hamilton CA, Kawahara AY, Sponberg S. 2021 Adaptive shifts underlie the divergence in wing morphology in bombycoid moths. *Proceedings of the Royal Society B: Biological Sciences* **288**.

6. Darveau CA. 2024 Insect Flight Energetics And the Evolution of Size, Form, And Function. *Integrative And Comparative Biology* **64**, 586–597.

7. Buchwald R, Dudley R. 2010 Limits to vertical force and power production in bumblebees (Hymenoptera: Bombus impatiens). *Journal of Experimental Biology* **213**, 426–432.

8. Wold ES, Aiello BR, Harris M, bin Sikandar U, Lynch J, Gravish N, Sponberg SN. 2024 Moth resonant mechanics are tuned to wingbeat frequency and energetic demands. *Proceedings of the Royal Society B: Biological Sciences* **291**.

9. Weis-Fogh T. 1973 Quick estimates of flight fitness in hovering animals, including novel mechanisms for lift production. *Journal of experimental Biology* **59**, 169–230.

10. Lynch J, Gau J, Sponberg S, Gravish N. 2021 Dimensional analysis of spring-wing systems reveals performance metrics for resonant flapping-wing flight. *Journal of the Royal Society Interface* **18**.

11. Gau J, Wold ES, Lynch J, Gravish N, Sponberg S, Sponberg S. 2022 The hawkmoth wingbeat is not at resonance. pp. 1–5.

12. Gau J, Gemilere R, Lds-Vip, Lynch J, Gravish N, Sponberg S. 2021 Rapid frequency modulation in a resonant system: Aerial perturbation recovery in hawkmoths. *Proceedings of the Royal Society B: Biological Sciences* **288**.

13. Pons A, Beatus T. 2022 Distinct forms of resonant optimality within insect indirect flight motors. *Journal of The Royal Society Interface* **19**.

14. Pons A. 2023 The self-oscillation paradox in the flight motor of D . melanogaster. *Arxiv*.

15. Jankauski MA. 2020 Measuring the frequency response of the honeybee thorax. *Bioinspiration and Biomimetics* **15**.

16. Sotavalta O. 1952 Flight-tone and wing-stroke frequency of insects and the dynamics of insect flight. *Nature* **170**, 1057–1058.

17. Weis-Fogh T. 1972 Energetics of Hovering Flight in Hummingbirds and in Drosophila. *Journal of Experimental Biology* **56**, 79–104.

18. Machin KE, Pringle JWS. 1959 The physiology of insect fibrillar muscle - II Mechanical properties of a beetle flight muscle. *Proceedings of the Royal Society of London. Series B. Biological Sciences* **151**, 204–225.

19. Josephson RK, Malamud JG, Stokes DR. 2000 Asynchronous muscle: A primer. *Journal of Experimental Biology* **203**, 2713–2722.

20. Gau J, Lynch J, Aiello B, Wold E, Gravish N, Sponberg S. 2023 Bridging two insect flight modes in evolution, physiology and robophysics. *Nature* **622**.

21. Josephson RK. 1997 Power output from a flight muscle of the bumblebee Bombus terrestris. III. Power during simulated flight. *Journal of Experimental Biology* **200**, 1241–1246.

22. Casey C, Heveran C, Jankauski M. 2023 Experimental studies suggest differences in the distribution of thorax elasticity between insects with synchronous and asynchronous musculature. *Journal of the Royal Society Interface* **20**.

23. Molloy JE, Kyrtatas V, Sparrow JC, White DC. 1988 Kinetics of flight muscles from insects with different wingbeat frequencies. *Nature* **328**, 449–451.

24. Swank DM. 2012 Mechanical analysis of Drosophila indirect flight and jump muscles. *Methods* **56**, 69–77.

25. Joos B, Young PA, Casey TM. 1991 Wingstroke frequency of foraging and hovering bumblebees in relation to morphology and temperature. *Physiological Entomology* **16**, 191–200.

26. Heinrich B. 1993 *The hot-blooded insects: strategies and mechanisms of thermoregulation*. Harvard University Press.

27. Gilmour KM, Ellington CP. 1993 in vivo Muscle Length Changes in Bumblebees and the in vitro Effects on Work and Power . *Journal of Experimental Biology* **183**, 101–113.

28. Pons A, Perl I, Ben-Dov O, Maya R, Beatus T. 2023 Solving the thoracic inverse problem in the fruit fly. *Bioinspiration and Biomimetics* **18**.

29. Tu MS, Daniel TL. 2004 Submaximal power output from the dorsolongitudinal flight muscles of the hawkmoth Manduca sexta. *Journal of Experimental Biology* **207**, 4651–4662.

30. Lynch J, Gau J, Sponberg S, Gravish N. 2022 Autonomous Actuation of Flapping Wing Robots Inspired by Asynchronous Insect Muscle. .

31. Salem W, Cellini B, Jaworski E, Mongeau JM. 2023 Flies adaptively control flight to compensate for added inertia. *Proceedings of the Royal Society B: Biological Sciences* **290**.

32. Harrison SM, Whitton RC, King M, Haussler KK, Kawcak CE, Stover SM, Pandy MG. 2012 Forelimb muscle activity during equine locomotion. *Journal of Experimental Biology* **215**, 2980–2991.

33. Westerga J, Gramsbergen A. 1993 Changes in the electromyogram of two major hindlimb muscles during locomotor development in the rat. *Experimental Brain Research* **92**, 479–488.

34. Dallmann CJ, Dürr V, Schmitz J. 2019 Motor control of an insect leg during level and incline walking. *Journal of Experimental Biology* **222**.

35. Gillis GB, Flynn JP, McGuigan P, Biewener AA. 2005 Patterns of strain and activation in the thigh muscles of goats across gaits during level locomotion. *Journal of Experimental Biology* **208**, 4599–4611.

36. Engberg I, Lundberg A. 1969 An Electromyographic Analysis of Muscular Activity in the Hindlimb of the Cat during Unrestrained Locomotion. *Acta Physiologica Scandinavica* **75**, 614–630.

37. Dickinson MH, Farley CT, Full RJ, Koehl MA, Kram R, Lehman S. 2000 How animals move: An integrative view. *Science* **288**, 100–106.

38. Josephson RK. 1985 Mechanical Power Output From Striated Muscle During Cyclic Contraction. *Journal of Experimental Biology* **114**, 493–512.

39. Anh A. 2012 How muscle function - the work loop technique. *Journal of Experimental Biology* **215**, 1051–1052.

40. Sponberg S, Abbott E, Sawicki GS. 2023 Perturbing the muscle work loop paradigm to unravel the neuromechanics of unsteady locomotion. *Journal of Experimental Biology* **226**.

41. Labonte D, Holt NC. 2022 Elastic energy storage and the efficiency of movement. *Current Biology* **32**, R661–R666.

42. Cavagna GA, Legramandi MA. 2015 Running, hopping and trotting: Tuning step frequency to the resonant frequency of the bouncing system favors larger animals. *Journal of Experimental Biology* **218**, 3276–3283.

43. Lehmann FO, Dickinson MH. 1997 The changes in power requirements and muscle efficiency during elevated force production in the fruit fly Drosophila melanogaster. *Journal of Experimental Biology* **200**, 1133–1143.

44. Loya AK, Van Houten SK, Glasheen BM, Swank DM. 2022 Shortening deactivation: quantifying a critical component of cyclical muscle contraction. *American Journal of Physiology - Cell Physiology* **322**, C653–C665.

45. Josephson RK, Malamud JG, Stokes DR. 2000 Power output by an asynchronous flight muscle from a beetle. *Journal of Experimental Biology* **203**, 2667–2689.

46. Melis JM, Siwanowicz I, Dickinson MH. 2023 Machine learning reveals the control mechanics of the insect wing hinge. *bioRxiv*.

47. Farisenkov SE, Kolomenskiy D, Petrov PN, Engels T, Lapina NA, Lehmann FO, Onishi R, Liu H, Polilov AA. 2022 Novel flight style and light wings boost flight performance of tiny beetles. *Nature* **602**, 96–100.

48. Wold ES, Liu E, Lynch J, Gravish N, Sponberg S. 2024 The Weis-Fogh Number Describes Resonant Performance Tradeoffs in Flapping Insects. *Integrative And Comparative Biology* **64**, 632–643.

49. Lynch J, Wold ES, Gau J, Sponberg SN, Gravish N. 2024 Energetic and control tradeoffs in spring-wing systems. *arXiv*.

50. Salem W, Cellini B, Kabutz H, Prasad HKH, Cheng B, Jayaram K, Mongeau JM. 2022 Flies trade off stability and performance via adaptive compensation to wing damage. *Science Advances* **8**, 1–12.

51. Pritchard DJ, Vallejo-Marín M. 2020 Floral vibrations by buzz-pollinating bees achieve higher frequency, velocity and acceleration than flight and defence vibrations. *Journal of Experimental Biology* **223**.

52. Dillon ME, Dudley R. 2014 Surpassing Mt. Everest: Extreme flight performance of alpine bumble-bees. *Biology Letters* **10**, 2–5.

53. Gilmour KM, Ellington CP. 1993 Power Output of Glycerinated Bumblebee Flight Muscle. *Journal of Experimental Biology* **183**, 77–100.

54. Lehmann FO, Skandalis DA, Berthé R. 2013 Calcium signalling indicates bilateral power balancing in the Drosophila flight muscle during manoeuvring flight. *Journal of the Royal Society Interface* **10**.

55. Wold ES, Lynch J, Gravish N, Sponberg S. 2023 Structural damping renders the hawkmoth exoskeleton mechanically insensitive to non-sinusoidal deformations. *Journal of the Royal Society Interface* **20**.

56. Gau J, Gravish N, Sponberg S. 2019 Indirect actuation reduces flight power requirements in Manduca sexta via elastic energy exchange. *Journal of the Royal Society Interface* **16**.

57. Dudek DM, Full RJ. 2006 Passive mechanical properties of legs from running insects. *Journal of Experimental Biology* **209**, 1502–1515.

58. Dickinson MH, Lehmann FO, Sane SP. 1999 Wing rotation and the aerodynamic basis of insect right. *Science* **284**, 1954–1960.

59. Han JS, Kim JK, Chang JW, Han JH. 2015 An improved quasi-steady aerodynamic model for insect wings that considers movement of the center of pressure. *Bioinspiration and Biomimetics* **10**.

60. Ellington CP. 1984 The aerodynamics of hovering insect flight. II. Morphological parameters. *Philosophical Transactions of the Royal Society of London. B, Biological Sciences* **305**, 17–40.

61. Whitney JP, Wood RJ. 2012 Conceptual design of flapping-wing micro air vehicles. *Bioinspiration and Biomimetics* **7**.

62. Josephson RK. 1997 Power output from a flight muscle of the bumblebee Bombus terrestris. III. Power during simulated flight. *Journal of Experimental Biology* **200**, 1241–1246.

63. Elliott SJ, Tehrani MG, Langley RS. 2015 Nonlinear damping and quasi-linear modelling. *Philosophical Transactions of the Royal Society A: Mathematical, Physical and Engineering Sciences* **373**.

64. Peckham M, Molloy JE, Sparrow JC, White DC. 1990 Physiological properties of the dorsal longitudinal flight muscle and the tergal depressor of the trochanter muscle of Drosophila melanogaster. *Journal of Muscle Research and Cell Motility* **11**, 203–215.

65. Chan WP, Dickinson MH. 1996 In vivo length oscillations of indirect flight muscles in the fruit fly Drosophila virilis. *Journal of Experimental Biology* **199**, 2767–2774.

66. King MJ, Buchmann SL, Spangler H. 1996 Activity of asynchronous flight muscle from two bee families during sonication (buzzing). *Journal of Experimental Biology* **199**, 2317–2321.

67. Dudley R, Ellington CP. 1990 Mechanics of Forward Flight in Bumblebees: I. Kinematics and Morphology. *Journal of Experimental Biology* **148**, 19–52.

68. Siomava N, Wimmer EA, Posnien N. 2016 Size relationships of different body parts in the three dipteran species Drosophila melanogaster, Ceratitis capitata and Musca domestica. *Development Genes and Evolution* **226**, 245–256.

69. Bullock SH. 1999 Relationships among Body Size , Wing Size and Mass in Bees from a Tropical Dry Forest in México Author (s): Stephen H . Bullock Source : Journal of the Kansas Entomological Society , Vol . 72 , No . 4 (Oct ., 1999), pp . 426-439 Published by : Allen P. *Journal of the Kansas Entomological Society* **72**, 426–439.

70. Pons A. 2024 Modelling rate-independent damping in insect exoskeleta via singular integral operators. *bioRxiv* pp. 1–31.

71. Weaver Jr W, Timoshenko SP, Young DH. 1991 *Vibration problems in engineering*. John Wiley & Sons.

72. Dickinson M, Farman G, Frye M, Bekyarova T, Gore D, Maughan D, Irving T. 2005 Molecular dynamics of cyclically contracting insect flight muscle in vivo. *Nature* **433**, 330–333.

73. Walker SM, Schwyn DA, Mokso R, Wicklein M, Müller T, Doube M, Stampanoni M, Krapp HG, Taylor GK. 2014 In Vivo Time-Resolved Microtomography Reveals the Mechanics of the Blowfly Flight Motor. *PLoS Biology* **12**.

74. Glasheen BM, Eldred CC, Sullivan LC, Zhao C, Reedy MK, Edwards RJ, Swank DM. 2017 Stretch activation properties of Drosophila and Lethocerus indirect flight muscle suggest similar calcium-dependent mechanisms. *American Journal of Physiology - Cell Physiology* **313**, C621–C631.

75. Fry SN, Sayaman R, Dickinson MH. 2005 The aerodynamics of hovering flight in Drosophila. *Journal of Experimental Biology* **208**, 2303–2318.